

Evaluation of algorithms for linear and nonlinear PID control for Twin Rotor MIMO System

Ricardo Cajo¹, Wilton Agila^{1,2}

¹Engineering Department, ²Electrical and Computer Engineering Department
¹Universidad Politécnica Salesiana (UPS), ²Escuela Superior Politécnica del Litoral (ESPOL)
 Guayaquil, Ecuador
 Email: ¹{rcajo,wagila}@ups.edu.ec, ²wagila@espol.edu.ec

Abstract— In this paper the linear and nonlinear PID control algorithms are analyzed and for a twin rotor MIMO system (TRMS), whose characteristic is not linear with two degrees of freedom and cross-links. The aim of this work is to stabilize the TRMS, to achieve a particular position and follow a trajectory in the shortest time. Mathematical modeling of helicopter model is simulated using MATLAB / Simulink, the two degrees of freedom are controlled both horizontally and vertically through the proposed controllers. Also nonlinear segmented observers for each degree of freedom are designed in order to measure statements required by the nonlinear controller. Followed, a comparative analysis of both algorithms is presented to evaluate their performance in the real TRMS.

Keywords — Twin Rotor MIMO System (TRMS); Proportional-Integral-Derivative (PID); Linear PID Controller; Nonlinear PID Controller; Nonlinear Observer.

I. INTRODUCTION

The Twin Rotor MIMO system 33-949S (TRMS) works as a model of a helicopter [1] and has two rotors, the main rotor allows vertical movement and is known as Pitch, while the secondary rotor or tail allows horizontal movement and is known as Yaw. Both are rotated by DC motors [2].

Traditional control scheme is based on the PID control technique which applies a signal to the process that is proportional to the drive signal and also adds integral and derived of drive signal. PID control algorithm is more often used in industrial control [3].

Several researchers have proposed various algorithms and control techniques based on: linear PID applied to each direct and cross-coupling variables [4], Fuzzy logic applied to the design of fuzzy controller and state observers [5-7], optimal state regulator [8], real value genetic algorithms (RGA) [9].

On this basis, this paper proposes a control algorithm known as nonlinear PID control based on classical tuning method of Ziegler and Nichols in frequency domain [10-11].

The rest of this article is organized as follows: Section II describes the mathematical model of TRMS. In section III the design of linear and nonlinear PID controllers are shown, in Section IV nonlinear observer is designed for both vertical and horizontal directions, then, in Section V, analysis of results and performance evaluation of control algorithms and dynamic

nonlinear observers is performed. Finally, conclusions are summarized in Section VI.

II. TRMS MODELING

The TRMS mechanical unit has two rotors placed on a beam, with a counterweight weighing arm which at its end is attached to the beam in the pivot and determines a stable equilibrium position as shown in Fig.1 [1].



Fig. 1. The twin rotor MIMO system

TRMS complete system dynamics can be well approximated in state space form as indicated in [12 -13] as follows:

$$\begin{aligned}
 \frac{d}{dt} \alpha_v &= \dot{\alpha}_v \\
 \frac{d}{dt} \dot{\alpha}_v &= \frac{a_1}{I_1} \tau_1^2 + \frac{b_1}{I_1} \tau_1 - \frac{M_g}{I_1} \sin \alpha_v + \frac{0.0326}{2I_1} \sin(2\alpha_v) (\dot{\alpha}_h)^2 \\
 &\quad - \frac{B_{1\alpha_v}}{I_1} \dot{\alpha}_v - \frac{k_{gy}}{I_1} a_1 \cos(\alpha_v) \dot{\alpha}_h \tau_1^2 - \frac{k_{gy}}{I_1} b_1 \cos(\alpha_v) \dot{\alpha}_h \tau_1 \\
 \frac{d}{dt} \alpha_h &= \dot{\alpha}_h \\
 \frac{d}{dt} \dot{\alpha}_h &= \frac{a_2}{I_2} \tau_2^2 + \frac{b_2}{I_2} \tau_2 - \frac{B_{1\alpha_h}}{I_2} \dot{\alpha}_h - \frac{1.75}{I_2} k_c a_1 \tau_1^2 - \frac{1.75}{I_2} k_c b_1 \tau_1 \\
 \frac{d}{dt} \tau_1 &= -\frac{T_{10}}{T_{11}} \tau_1 + \frac{k_1}{T_{11}} u_1 \\
 \frac{d}{dt} \tau_2 &= -\frac{T_{20}}{T_{21}} \tau_2 + \frac{k_2}{T_{21}} u_2
 \end{aligned} \tag{1}$$

III. DESIGN OF PID CONTROLLERS

Output is described by:

$$y = [\alpha_v \ \alpha_h]^T \quad (2)$$

Where,

- α_v : Pitch (elevation) angle
- α_h : Yaw (azimuth) angle
- τ_1 : Momentum of main rotor
- τ_2 : Momentum of tail rotor
- u_1 : Control signal of main rotor
- u_2 : Control signal of tail rotor

To facilitate identification of each physical sign of TRMS $[\alpha_v \ \dot{\alpha}_v \ \alpha_h \ \dot{\alpha}_h \ \tau_1 \ \tau_2]$ we will use each state's representation $[x_1 \ x_2 \ x_3 \ x_4 \ x_5 \ x_6]$ respectively.

A. Vertical subsystem model (pitch)

Through the analysis of relative gain array (RGA), the interaction between inputs and outputs is low so we will approach the representation (1) only for the states involved in the vertical output (α_v), when $u_2 = 0$ we have the representation in state space for the pitch $[x_1 \ x_2 \ x_5]$.

$$\begin{aligned} \frac{d}{dt} x_1 &= x_2 \\ \frac{d}{dt} x_2 &= \frac{a_1}{I_1} x_5^2 + \frac{b_1}{I_1} x_5 - \frac{Mg}{I_1} \sin x_1 - \frac{B_1 \alpha_v}{I_1} x_2 \\ \frac{d}{dt} x_5 &= -\frac{T_{10}}{T_{11}} x_5 + \frac{k_1}{T_{11}} u_1 \\ y &= [x_1]^T \end{aligned} \quad (3)$$

B. Horizontal subsystem model (yaw)

Like in the pitch subsystem, we will approach the representation (1) only for the states involved in the horizontal output (α_h), when $u_1 = 0$ we have the representation in state space for the yaw subsystem $[x_3 \ x_4 \ x_6]$.

$$\begin{aligned} \frac{d}{dt} x_3 &= x_4 \\ \frac{d}{dt} x_4 &= \frac{a_2}{I_2} x_6^2 + \frac{b_2}{I_2} x_6 - \frac{B_1 \alpha_h}{I_2} x_4 \\ \frac{d}{dt} x_6 &= -\frac{T_{20}}{T_{21}} x_6 + \frac{k_2}{T_{21}} u_2 \\ y &= [x_3]^T \end{aligned} \quad (4)$$

In this section, the design of linear and nonlinear PID controllers is done, for this, each controller is divided in two parts.

A. Design of linear PID controller for pitch subsystem

To design the first linear controller, it is required to linearize the model shown in (3), for that, its parameterized balance point relative to the input $u_1 = U_1$ is calculated. As it's indicated in (5).

$$\begin{aligned} x_1 &= X_1(U_1) = \arcsin\left[\frac{k_1}{MgT_{10}} \left(\frac{a_1 k_1}{T_{10}} U_1^2 + b_1 U_1\right)\right] \\ x_2 &= 0 \quad x_5 = X_5(U_1) = \frac{k_1}{T_{10}} \end{aligned} \quad (5)$$

The linearized model in state space is shown in (6).

$$A_v = \begin{bmatrix} 0 & 1 & 0 \\ \lambda & \beta & \gamma \\ 0 & 0 & \theta \end{bmatrix} \quad B_v = \begin{bmatrix} 0 \\ 0 \\ \rho \end{bmatrix} \quad C_v = [1 \ 0 \ 0] \quad D_v = 0 \quad (6)$$

Where,

$$\begin{aligned} \lambda &= -\frac{Mg}{I_1} \cos X_1(U_1) & \beta &= -\frac{B_1 \alpha_v}{I_1} \\ \theta &= \frac{-T_{10}}{T_{11}} & \gamma &= \frac{2a_1}{I_1} X_5(U_1) + \frac{b_1}{I_1} & \rho &= \frac{k_1}{T_{11}} \end{aligned} \quad (7)$$

Another way to express the model (6), is by its transfer function, given in (8).

$$G_{U_1}(s) = \frac{\rho \gamma}{s^3 - s^2(\beta + \theta) + s(\theta\beta - \lambda) + \theta\lambda} \quad (8)$$

The adjustment of PID parameters is done in MATLAB / Simulink using the LGR method.

B. Design of linear PID controller for yaw subsystem

The parameterized balanced point relative to input $u_2 = U_2$ is shown in (9).

$$x_3 = X_3(U_2) = 0 \quad x_4 = 0 \quad x_6 = X_6(U_2) = \frac{k_2}{T_{20}} U_2 \quad (9)$$

The linearized model in state space is shown in (10).

$$A_h = \begin{bmatrix} 0 & 1 & 0 \\ 0 & R & \sigma \\ 0 & 0 & \phi \end{bmatrix} \quad B_h = \begin{bmatrix} 0 \\ 0 \\ \phi \end{bmatrix} \quad C_h = [1 \ 0 \ 0] \quad D_h = 0 \quad (10)$$

Where,

$$\begin{aligned} R &= -\frac{B_1\alpha_h}{I_2} & \Omega &= \frac{-T_{20}}{T_{21}} \\ \sigma &= \frac{2a_2}{I_2} X_6(U_2) + \frac{b_2}{I_2} & \phi &= \frac{k_2}{T_{21}} \end{aligned} \quad (11)$$

Another way to express the model (10), is by its transfer function, given in (12).

$$G_{U_2}(s) = \frac{\phi\sigma}{s^3 - s^2(R + \Omega) + s(R\Omega)} \quad (12)$$

The adjustment of PID parameters is done in MATLAB / Simulink using the LGR method.

C. Design of nonlinear PID controller for pitch subsystem

On the Ziegler-Nichols method of critical response in frequency domain, system Parameters $P_0(U_1) K_0(U_1)$ are determined, these values are calculated analytically from the transfer function $G_{U_1}(s)$ where it is obtained that:

$$P_0(U_1) = \frac{2\pi}{\sqrt{\theta\beta - \lambda}} K_0(U_1) = \left| \frac{\beta(\theta^2 + \theta\beta - \lambda)}{\rho\gamma} \right| \quad (13)$$

The generalized nonlinear PID controller takes the following form:

$$\begin{aligned} \dot{z}_v(t) &= 7.74 \frac{K_0(z_v(t))}{P_0(z_v(t))} (\text{Ref} - x_1(t)) \\ u_1(t) &= z_v(t) + 0.0372 K_0(z_v(t)) (\text{Ref} - x_1(t)) \\ &\quad - 0.5837 K_0(z_v(t)) P_0(z_v(t)) x_2(t) \end{aligned} \quad (14)$$

Where $z_v(t)$ is defined as a state of the vertical non-linear controller. The control signal $u_1(t)$ will require the states $x_1(t), x_2(t)$ of which in the real TRMS system currently only states $x_1(t)$ y $x_3(t)$ can be measured, therefore we need to estimate the state $x_2(t)$.

D. Design of nonlinear PID controller for yaw subsystem

Like the design made in paragraph C, parameters $P_0(U_2) K_0(U_2)$ will be determined, these values are calculated analytically from the transfer function $G_{U_2}(s)$ where it is obtained that:

$$P_0(U_2) = \frac{2\pi}{\sqrt{R\Omega}} K_0(U_2) = \left| \frac{R\Omega(R + \Omega)}{\phi\sigma} \right| \quad (15)$$

The generalized nonlinear PID controller takes the following form:

$$\begin{aligned} \dot{z}_h(t) &= 1.42 \frac{K_0(z_h(t))}{P_0(z_h(t))} (\text{Ref} - x_3(t)) \\ u_2(t) &= z_h(t) + 0.0984 K_0(z_h(t)) (\text{Ref} - x_3(t)) \\ &\quad - 0.0285 K_0(z_h(t)) P_0(z_h(t)) x_4(t) \end{aligned} \quad (16)$$

Where $z_h(t)$ is defined as a state of the vertical non-linear controller. The control signal $u_2(t)$ will require the states $x_3(t), x_4(t)$ of which in the real TRMS system currently only states $x_1(t)$ y $x_3(t)$ can be measured, therefore we need to estimate the state $x_4(t)$.

IV. DESIGN OF STATE OBSERVERS

Here, the nonlinear dynamic observers based on Luenberger observer are designed.

A. Design of nonlinear observer for pitch subsystem

We start from Luenberger's linear observer whose general structure in closed loop is given by:

$$\begin{aligned} \dot{\hat{x}} &= A\hat{x}_\delta + Bu_\delta + L(y_\delta - \hat{y}_\delta) \\ &= (A - LC)\hat{x}_\delta + Bu_\delta + LC\hat{x}_\delta \\ \hat{y}_\delta &= C\hat{x}_\delta \end{aligned} \quad (17)$$

Where vector $L_v \in \mathfrak{R}^{3 \times 1}$ being the solution of (17) satisfies the following condition:

$$\det(sI - A_v + L_v C_v) = \text{selected_polynomial_pitch} \quad (18)$$

For which the following polynomial is selected:

$$s^3 + 14s^2 + 44s + 40 \quad (19)$$

Using (18) and (19) it is determined that L is:

$$\begin{aligned} L_1 &= 14 + \theta + \beta \\ L_2 &= 44 - \lambda + L_1(\theta + \beta) - \theta\beta \\ L_5 &= \frac{40 + \theta(L_2 - \lambda) - L_1\theta\beta}{\gamma} \end{aligned} \quad (20)$$

Once the vector L_v is calculated, Next step is to extend the model (17) to nonlinear case with the form:

$$\begin{aligned}\dot{\hat{x}}(t) &= f(\hat{x}(t), u_1(t)) + B_v u_1(t) + g(y(t)) - g(\hat{y}(t)) \\ \hat{y}(t) &= h\hat{x}(t)\end{aligned}\quad (21)$$

Where $\left. \frac{dg(y(t))}{dy} \right|_{y=X_1(U_1)} = L_v(U_1)$ with which we obtain:

$$\begin{aligned}g_1(y) &= (14 + \theta + \beta)y \\ g_2(y) &= (44 + L_1(\theta + \beta) - \theta\beta)y - \frac{M_g}{I_1} \cos(y) \\ g_5(y) &= \int \frac{I_1(40 + 44\theta - L_1\theta^2 - \theta^2\beta)}{\sqrt{b_1^2 + 4a_1M_g} \sin y} dy\end{aligned}\quad (22)$$

B. Design of nonlinear observer for yaw subsystem

Similarly to the design made in A, the structure given in (17) is used, next, the vector $L_h \in \mathfrak{R}^{3 \times 1}$ is calculated so that the solution must satisfy the following condition:

$$\det(sI - A_h + L_h C_h) = \text{selected_polynomial_yaw} \quad (23)$$

For which the following polynomial is selected:

$$s^3 + 13s^2 + 32s + 20 \quad (24)$$

Using (23) and (24) it is determined that L_h is:

$$\begin{aligned}L_3 &= 13 + R + \Omega \\ L_4 &= 32 + L_3(R + \Omega) - R\Omega \\ L_6 &= \frac{L_3 R \Omega - L_4 \Omega - 20}{\sigma}\end{aligned}\quad (25)$$

Once the vector L_h was found, next step is to extend the model (17) to the nonlinear case with the form:

$$\begin{aligned}\dot{\hat{x}}(t) &= f(\hat{x}(t), u_2(t)) + B_h u_2(t) + g(y(t)) - g(\hat{y}(t)) \\ \hat{y}(t) &= h\hat{x}(t)\end{aligned}\quad (26)$$

Where $\left. \frac{dg(y(t))}{dy} \right|_{y=X_2(U_2)} = L_h(U_2)$ with which we obtain that:

$$\begin{aligned}g_3(y) &= (13 + R + \Omega)y \\ g_4(y) &= (32 + L_3(R + \Omega) - R\Omega)y \\ g_6(y) &= \frac{L_3 R \Omega - L_4 \Omega - 20}{2a_2 X_6(U_2) + \frac{b_2}{I_2}} y\end{aligned}\quad (27)$$

V. PERFORMANCE EVALUATION

System parameters of the TRMS are seen in Table I.

TABLE I: TRMS parameters [1]

Parameters	Values
I_1 - Moment of inertia of vertical rotor	$6.8 \cdot 10^{-2} \text{ kg} \cdot \text{m}^2$
I_2 - Moment of inertia of horizontal rotor	$2 \cdot 10^{-2} \text{ kg} \cdot \text{m}^2$
a_1 - Static characteristic parameter	0.0135
b_1 - Static characteristic parameter	0.081
a_2 - Static characteristic parameter	0.02
b_2 - Static characteristic parameter	0.09
M_g - Gravity momentum	0.32 N.m
$B_{1\alpha_v}$ - Friction momentum function parameter	$6 \cdot 10^{-3} \text{ N} \cdot \text{m} \cdot \text{s} / \text{rad}$
$B_{2\alpha_v}$ - Friction momentum function parameter	$1 \cdot 10^{-3} \text{ N} \cdot \text{m} \cdot \text{s}^2 / \text{rad}$
$B_{1\alpha_h}$ - Friction momentum function parameter	$1 \cdot 10^{-1} \text{ N} \cdot \text{m} \cdot \text{s} / \text{rad}$
$B_{2\alpha_h}$ - Friction momentum function parameter	$1 \cdot 10^{-2} \text{ N} \cdot \text{m} \cdot \text{s}^2 / \text{rad}$
k_{gy} - Gyroscopic momentum parameter	0.05 s/rad
k_1 - Motor 1 gain	1.1
k_2 - Motor 2 gain	0.8
T_{11} - Motor 1 denominator parameter	1.1
T_{10} - Motor 1 denominator parameter	1
T_{21} - Motor 2 denominator parameter	1
T_{20} - Motor 2 denominator parameter	1
T_p - Cross reaction momentum parameter	2
T_0 - Cross reaction momentum parameter	3.5
k_c - Cross reaction momentum gain	-0.2

The bound for control signal is set to $-2.5V \dots + 2.5V$, [1].

These parameters are used in the evaluation of observers and PID controllers made in MATLAB / Simulink and discussed in section A, B, C and D.

A. Evaluation of nonlinear observer for pitch subsystem

The system is operated in open loop with initial conditions set to zero for both the system and the observer. Control signals $u_1(t) = 1.6$ and $u_2(t) = 0$ are applied for the main and tail rotors respectively, the response of the current state and the observed are shown in Figure 2, which shows the good performance of the estimator, the error between the current state and the estimated for the pitch angle is bounded within a small region around zero. Note that the efficiency of the observer depends on model accuracy.

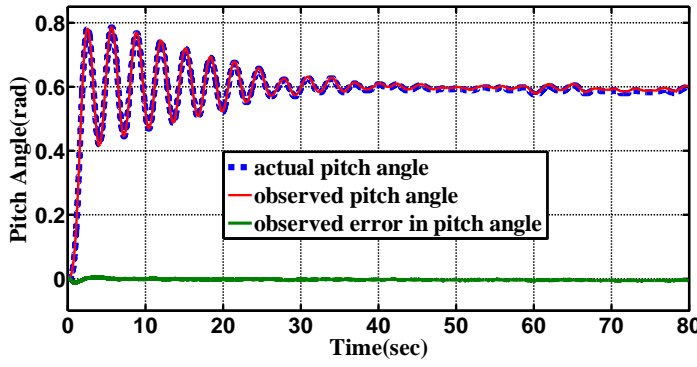


Fig. 2. Current state, estimated state and estimation error for pitch angle.

B. Evaluation of nonlinear observer for yaw subsystem

Following the evaluation of the system in open loop, now for control signals $u_1(t) = 0$ y $u_2(t) = 0.8$ for main and tail rotors respectively, initial conditions for both the system and the observer are set to zero. The response of the current state and the observed are shown in Figure 3, which shows the good performance of the estimator.

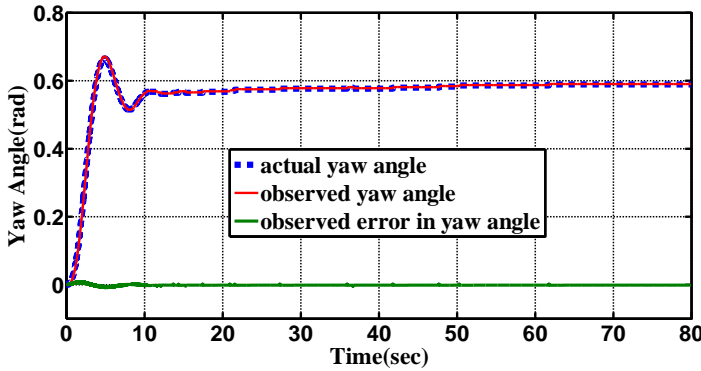


Fig. 3. Current state, estimated state and estimation error for yaw angle.

C. Evaluation of linear and nonlinear PID controller for pitch subsystem.

Step response of vertical angle is shown in Fig.4, where it is obtained a stabilization time $t_s = 10.3$ sec for both controllers, nevertheless the linear PID controller shows an overshoot of 6%.

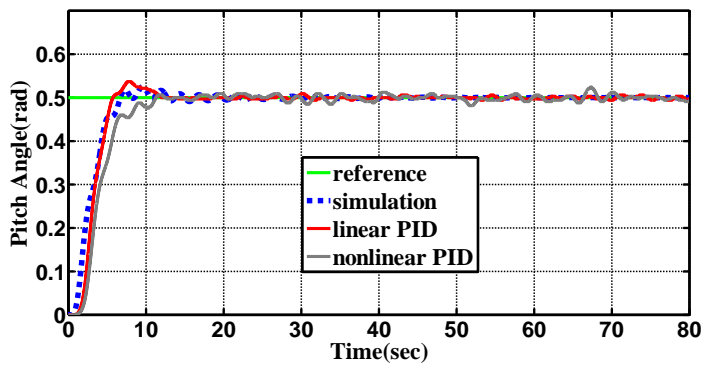


Fig. 4. Step response of the vertical angle.

The comparison between the control signals of both PID is shown in Fig.5, where it is evidenced a better performance of the nonlinear PID due to having a signal free of peaks, which are not favorable for the actuator.

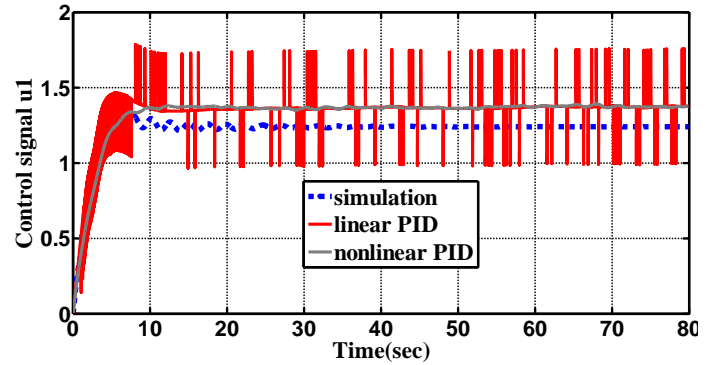


Fig. 5. Control signal $u_1(t)$ of PID controller.

D. Evaluation of linear and nonlinear PID controller for yaw subsystem.

In Fig.6 it is shown the step response of the horizontal angle, where it is obtained a stabilization time $t_s = 8.2$ sec for the linear PID, whilst the nonlinear shows a stabilization time $t_s = 16.1$ sec and overshoot of 18%.

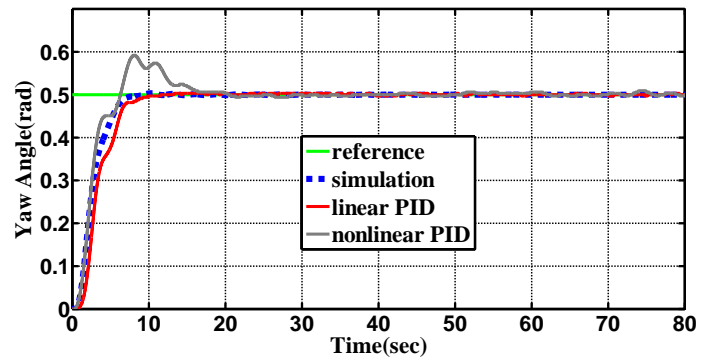


Fig. 6. Step response of horizontal angle.

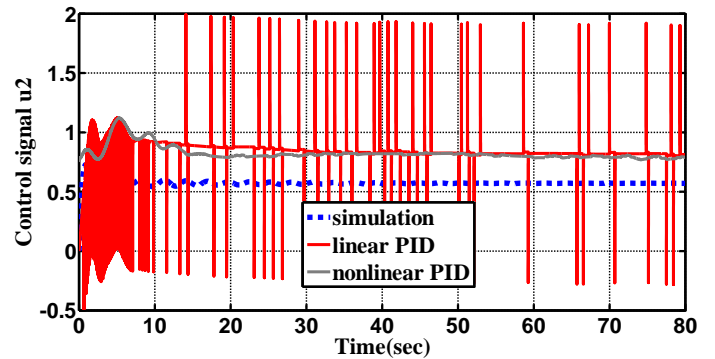


Fig. 7. Control signal $u_2(t)$ of PID controller

Although the temporal response of the linear controller turns out to be better in Fig.7 control signals of both controllers are analyzed where it is observed that the nonlinear PID has greater energy efficiency.

E. Evaluation of linear and nonlinear PID controllers for TRMS

After the evaluation made to each controller independently, Fig.8 shows the result of both controllers working together where appropriate monitoring of both references in the vertical and horizontal angle is observed respectively.

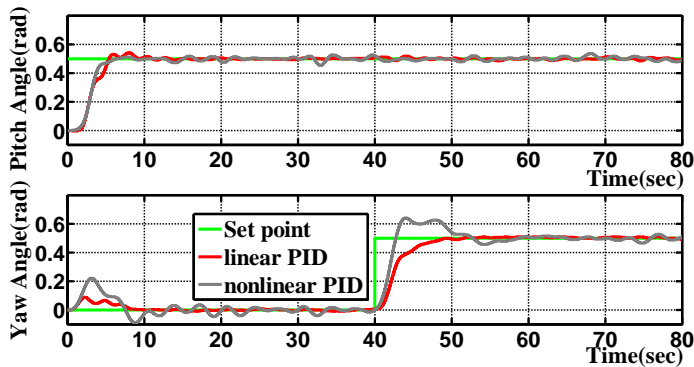


Fig. 8. Step response of vertical and horizontal angle.

VI. CONCLUSIONS

In this paper, stabilizing at a particular position and effective follow of a trajectory is implemented through linear and nonlinear algorithms applied to TRMS. The results show that both controllers stabilize the system, but the nonlinear controller has better performance in terms of energy because their control signals are of lower amplitude peaks and thus the life of the actuators is protected.

ACKNOWLEDGEMENT

The authors thank to Universidad Politécnica Salesiana-Sede Guayaquil and his research group in control systems (GISCOR) for allowing the use of TRMS automatic control laboratory.

REFERENCES

- [1] TRMS 33-949S User Manual, Feedback instruments Ltd., East Sussex, U.K.
- [2] Prasad, D.G.; Manoharan, P.S.; Ramalakshmi, A.P.S., "PID control scheme for twin rotor MIMO system using a real valued genetic algorithm with a predetermined search range," Power, Energy and Control (ICPEC), 2013 International Conference on, vol., no., pp.443,448, 6-8 Feb. 2013.
- [3] A. Odwyer, Handbook of PI and PID Controller Tuning Rules. London, U.K.: Imperial College Press, 2003.
- [4] A. Ramalakshmi and P. Manoharan, "Non-linear modeling and PID control of twin rotor MIMO system," in IEEE Conference on Advanced Communication Control and Computing Technologies, 2012, pp. 366–369.
- [5] Islam, B.U.; Ahmed, N.; Bhatti, D.L.; Khan, S., "Controller design using fuzzy logic for a twin rotor MIMO system," Multi Topic Conference, 2003. INMIC 2003. 7th International, vol., no., pp.264,268, 8-9 Dec. 2003
- [6] Saroj, D.K.; Kar, I., "T-S fuzzy model based controller and observer design for a Twin Rotor MIMO System," Fuzzy Systems (FUZZ), 2013 IEEE International Conference on, vol., no., pp.1,8, 7-10 July 2013
- [7] Rahideh, A.; Shaheed, M.H., "Hybrid Fuzzy-PID-based Control of a Twin Rotor MIMO System," IEEE Industrial Electronics, IECON 2006 - 32nd Annual Conference on, vol., no., pp.48,53, 6-10 Nov. 2006.
- [8] Pratap, B.; Agrawal, A.; Purwar, S., "Optimal control of twin rotor MIMO system using output feedback," Power, Control and Embedded Systems (ICPCES), 2012 2nd International Conference on, vol., no., pp.1,6, 17-19 Dec. 2012
- [9] Jih-Gau Juang; Ming-Te Huang; Wen-Kai Liu, "PID Control Using Presearched Genetic Algorithms for a MIMO System," Systems, Man, and Cybernetics, Part C: Applications and Reviews, IEEE Transactions on, vol.38, no.5, pp.716,727, Sept. 2008
- [10] B. C. Kuo, *Automatic Control Systems*, 6th ed. Englewood Cliffs, NJ: Prentice-Hall, 1995.
- [11] J. G. Ziegler and N. B. Nichols, "Optimum settings for automatic controllers," *Trans. ASME*, vol. 64, pp. 759–768, Nov. 1942.
- [12] Pratap, B.; Purwar, S., "Sliding mode state observer for 2-DOF twin rotor MIMO system," Power, Control and Embedded Systems (ICPCES), 2010 International Conference on, vol., no., pp.1,6, Nov. 29 2010-Dec. 1 2010
- [13] Pratap, B.; Purwar, S., "State observer based robust feedback linearization controller for twin rotor MIMO system," Control Applications (CCA), 2012 IEEE International Conference on, vol., no., pp.1074,1079, 3-5 Oct. 2012.